Microphase Structure of Block Ionomers. 3. A SAXS Study of the Effects of Architecture and Chemical Structure

Jean-Pierre Gouin,† Francis Bossé,† Diep Nguyen,† Claudine E. Williams,*,‡ and Adi Eisenberg*,†

Department of Chemistry, McGill University, Montréal, Québec, Canada H3A 2K6, and Laboratoire pour l'Utilisation du Rayonnement Électromagnétique (LURE), CNRS–CEA–MEN, Université Paris-Sud, 91405 Orsay Cedex, France

Received February 24, 1992; Revised Manuscript Received April 6, 1993®

ABSTRACT: The structure of various ionic block copolymers of ABA and AB architecture was investigated by small-angle X-ray scattering (SAXS). Polystyrene formed the B-blocks of all materials, and vinylpyridinium methyl iodide or cesium methacrylate formed the ionic A blocks. The latter were kept short and spherical ionic domains were observed. The morphology was studied as a function of the lengths of both ionic and nonionic blocks and of the methods of preparation (neutralization in different solvents, solvent casting, or compression molding). A strong correlation peak was observed, often followed by features related to shape factors for the spherical microdomains. The radii calculated from these two different features are in good agreement. In was concluded that, within experimental error, the size of the ionic microdomains is independent of the length of the nonionic block, the chemical structure of the ionic block, the method of preparation, or the architecture. The ionic segments are highly extended in their microdomains.

Introduction

The present paper deals with block copolymers consisting of short ionic and long nonionic segments. These are of interest because they combine the properties of ionomers on the one hand and block copolymers on the other. Ionomers have been, and still are, of interest from both the academic and industrial point of view. The most common, and also the first to be studied, are the random ionomers, in which the ions are distributed statistically along the polymer chain.[1–7] In bulk or in nonpolar solvents, ionic aggregation produces physical cross-links (multiplets) which are responsible for the major modification in the properties of the material, even when only a few percent of ionic groups are present.

Block copolymers represent another area of interest from many points of view.[8–14] Here, it is the incompatibility between the different blocks that results in phase-separated microdomains which, in turn, are responsible for the special properties of these materials. The microdomains are lamellar, cylindrical, or spherical, depending on the relative volume content of the different blocks: in the latter case, corresponding to a low volume fraction, these also act as physical cross-links of a 3-D network. Because of the joint effects of dipolar attraction of the ionic groups and strong incompatibility between the segments, block ionomers phase separate, even for very short block lengths. The limiting case is that of halato-telechelics in which one ion pair is placed at each end of short polymer chains. In these materials, the ion pairs have been found to aggregate into multiplets with a liquid-like order in the organic matrix.[15]

Recently, AB, ABA, and star block ionomers characterized by long nonionic blocks and relatively short ionic sequences were synthesized in different laboratories.[16–27] In solution, the marked differences in the solvation properties of the ionic and nonionic sequences result in materials with colloidal properties.[28–30] In the solid state, the mechanical properties[19,22] are characterized by a broad rubbery plateau, a high modulus, and a high tensile strength. All these properties can be related to microphase separation between ionic and nonionic moieties in the material. A recent SAXS investigation of the bulk morphology of an ABA poly(styrene–methyl vinylpyridinium) block ionomer[27] has confirmed the presence of ionic domains. The short ionic sequences were found to be highly elongated in their microphase. It was also concluded that, due to the method of preparation, the ionic domains had the shape of deformed spheres, being either short cylinders or small disks. The polystyrene (PS) segment was found to have its unperturbed dimensions as determined by SANS.[31] The morphology of ABA styrene–alkyl vinylpyridinium copolymers, where the alkyl chain varied from ethyl to decyl, was also examined by SAXS.[32] Two types of scattering patterns were observed, depending on the architectural features of the materials.

SAXS and TEM are techniques most commonly used to characterize the structure of microphase-separated materials. However, it should be pointed out that neither technique has been successful in assessing the structure of most types of ionomers, because of the low ion contents of these materials and the lack of long-range order in the distribution of the ionic aggregates. For this investigation, we have chosen to use SAXS because the experimental scattering profiles show more features than the broad peak, sometimes followed by a weak shoulder, characteristic of the common random ionomers and the telechelics.

This paper presents the results of a morphological investigation of polystyrene-based block ionomers with very short ionic blocks of 10–50 monomers displaying spherical morphology. The effect of various factors was investigated, including the architecture (AB, ABA), the method of preparation (compression molding, solvent casting, and neutralization in different solvents), the chemical nature of the ionic segment (cesium methacrylate, vinylpyridinium methyl iodide), and the molecular weight of the ionic and the nonionic sequences.

Experimental Section

Materials. The preparation of the materials has been described elsewhere.[19,33] Thus, only a summary of the procedure will be given here. The block copolymers were synthesized by sequential anionic copolymerization. A specially designed polymerization line allows the synthesis of a series of block

† McGill University.
‡ Université Paris-Sud.
® Abstract published in *Advance ACS Abstracts*, November 1, 1993.

0024-9297/93/2226-7250$04.00/0

copolymers with identical nonionic block lengths and different ionic block lengths. Different series of samples were prepared with polystyrene blocks of molecular weight ranging from 20 000 to 100 000 (200 to 1000 units) and with vinylpyridine or *tert*-butyl methacrylate blocks ranging from 1000 to 5000 (10 to 50 units). In the case of AB materials the initiator used was *n*-butyllithium, while for ABA materials the sodium–naphthalene complex was used.

For the vinylpyridine (4VP) materials, the pyridine content of the copolymers were determined by FTIR for the samples containing less than 10 mol % of vinylpyridine. Nonaqueous titration of the vinylpyridine segments by perchloric acid was performed for all samples except for the series of ABA materials with polystyrene blocks of molecular weight 100 000, since gelation occurred after only a few milliliters of titrant had been added. For the methacrylate materials, the catalyzed hydrolysis gave the corresponding methacrylic acid materials. The acid content was determined by nonaqueous titration. The molecular weights of the polystyrene blocks were determined by size exclusion chromatography (SEC). The resulting precision on the number of repeat units per block is of the order of 5%. The polydispersity index was found to vary from 1.1 to 1.3 for the samples used in this study.

The nonionic vinylpyridine copolymers were compression molded at ca. 130 °C and soaked in 80/20 (v/v) absolute ethanol/methyl iodide solution for 3 days under reflux to quaternize the 4VP units. Under these conditions, the polystyrene matrix is swollen by the methyl iodide. The samples were then dried under vacuum at 110 °C. The disappearance of the 1414-cm^{-1} 4VP IR band was taken as evidence of complete quaternization. These samples were dissolved to produce 3% w/w solutions in either in dimethylformamide (DMF) or in an equimolar mixture of DMF/cyclohexanone. These solutions were evaporated under a reduced pressure of 0.5 atm at room temperature over a period of ca. 1 week. Further drying was achieved by placing the samples for 2 days in a vacuum oven under reduced pressure at 110 °C.

The methacrylic acid copolymers were neutralized with cesium hydroxide in dioxane or in a 80/20 v/v benzene/methanol mixture. The resulting solutions were either evaporated under ambient conditions or freeze-dried. The freeze-dried powder was either compression molded at 140 °C or dissolved in various solvents and allowed to evaporate under a pressure of 0.5 atm at room temperature. Table I lists all of the materials, along with the methods of preparation used for each of the samples.

Small-Angle X-ray Scattering. The experiments used in synchrotron as a source of radiation (LURE DCI storage ring, Orsay). The spectrometer[34] is equipped with a double-crystal, fixed-exit monochromator providing a beam of narrow energy range (resolution ≅ 0.1%) tunable from 4 to 15 keV (3–0.8 Å). A wavelength of 1.46 Å was used for these experiments. The size of the beam at the sample was ca. 1 mm^2. The scattered radiation was detected with a gas-filled one-dimensional position-sensitive detector with a resolution of 135 μm. To reduce background noise, the beam path, including the sample, was kept in vacuum. The angular range was chosen to provide data extending from $q = 0.005$ to 0.21 $Å^{-1}$, where $q = 4\pi \sin\theta/\lambda$, and θ is one-half the scattering angle. The resulting I vs q curves were corrected for incident beam decay, sample thickness, and transmission. The background scattering from a polystyrene homopolymer or an empty sample holder was subtracted. The optics of the experimental setup was such that no desmearing of the curves was necessary.

Results and Discussion

Two types of scattering patterns were obtained, as illustrated in Figure 1. The first type consists of a broad, asymmetric peak. These logarithmic plots revealed the presence of a weak shoulder at larger angles. While this feature is broad and not intense, it was frequently possible to assign this feature to a shape factor for spheres. However, no structural information (beyond the value of the radius) could be obtained. This type of pattern was generally characteristic of ABA materials that were prepared by compression molding and was described in some detail in paper 1 of this series.[27] The second type of pattern is much more complex: a sharp and symmetric peak, often accompanied by a second-order feature, was observed in all samples and was generally followed by well-defined intensity maxima at higher q values. This kind of scattering pattern is typical of solvent cast ABA materials and of AB blocks prepared by the different methods listed in Table I. It will be discussed in more detail below.

For an assembly of centroasymmetric particles, the resulting scattered intensity $I(q)$ is the *product* of the form factor for isolated particles, $P(q)$, and the structure factor, $S(q)$, which characterizes their spatial correlations. Sorting out the origin of the various peaks cannot be done

Table I. Bragg Distances[a] (Å)

samples	preparation method[b] 1	2	3	4
4VP·MeI–Styrene				
13–260[c]	258	192		
29–260	357	242		
71–260	469	357		
10–200–10	128	144		
20–200–20	153	138		
48–200–48	170	258		
9–480–9	157	163		
17–480–17	180	178		
48–480–48	217	220		
12–960–12	209	227		
24–960–24	262	242		
36–960–36	299	253		
48–960–48	299	267		
CsMA–Styrene Neutralized in Dioxane				
7–440	196	234	190	174
18–440	208	214	197	208
39–440	258	258	234	311
8–490–8			163	187
22–490–22			192	277
44–490–44				393
CsMA–Styrene Neutralized in Benzene/MeOH				
7–440		183		197
18–440		227		249
39–440		277		299
8–490–8				197
22–490–22				277
44–490–44				258

[a] Bragg distance = $2\pi/q_{max}$. [b] 1, DMF casting; 2, DMF/cyclohexanone casting; 3, evaporated from the neutralization solution; 4, freeze-drying and compression molding. [c] Lengths of the A and B blocks in number of repeat units; A blocks are ionic, and the B blocks are polystyrene.

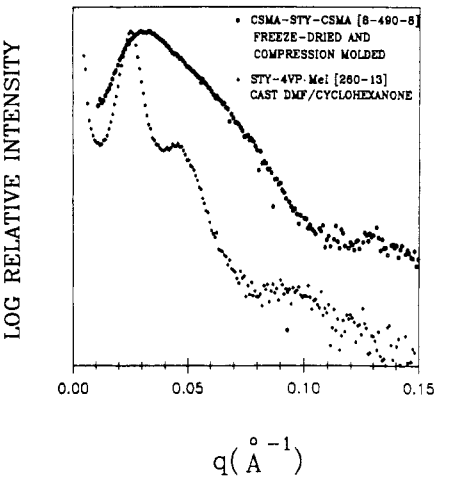

Figure 1. The two types of observed scattering patterns.

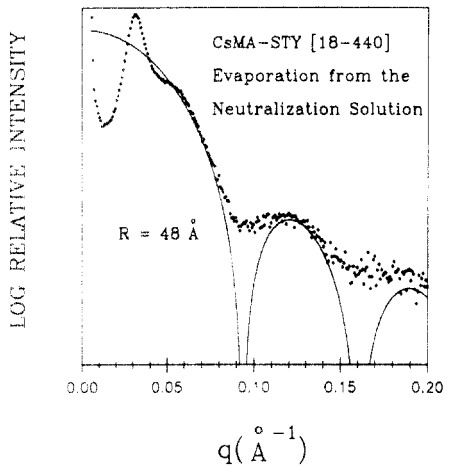

Figure 2. Scattering profile for the $P(S_{440}$-b-$CsMA_{18})$ sample, with a clear shape factor at larger angles. The calculated shape factor curve for monodisperse spheres is shown as a continuous line (eq 2 with R = 48 Å).

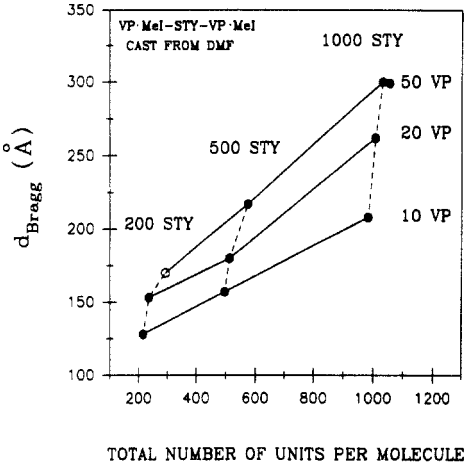

Figure 3. Variation of the Bragg distance as a function of the length of the ionic and the nonionic blocks for a set of 4VP–PS–4VP samples. Solid lines connect samples of similar numbers of 4VP units, and dashed lines connect samples of identical number of styrene units. The labels are rounded to one significant figure (see the tables for precise listings). The point for the 48–200–48 sample (open circle) may not correspond to the same morphology as the others and has not been considered further.

unambiguously without assumptions concerning the morphology. By comparison with the known structure of telechelic ionomers[35] and nonionic block copolymers, the ionic domains were assumed to be small and dispersed in the PS matrix with some position correlation. Hence, the first narrow peak was attributed to an interparticle correlation function, and Bragg's law was applied to deduce a characteristic distance, d_{Bragg}. The subsequent peaks are broad and less intense. They may be related to higher order structure factors or to shape factors of the ionic domains. Swelling of the PS with a nonpolar solvent, which should not affect the ionic phase, was decisive for the attribution; it resulted in a displacement of the correlation peak to lower angles whereas those peaks situated at wider angles remained unchanged; therefore, they were attributed to shape factors for approximately spherical objects. Attribution schemes other than those adopted here led to characteristic distances that were not compatible with the molecular characteristics of the samples.

At this point, a few remarks are called for. First, for a given radius value and a well-defined shape, it is possible to calculate the shape factor pattern. A typical plot obtained for a sphere (see eq 2, discussed below) is illustrated in Figure 2 for $P(S_{440}$-b-$CsMA_{18})$. As seen in this figure, the shape factors are quite smeared out, by comparison with the calculated shape factor for monodisperse spheres of R = 48 Å (see below). This indicates either that the domains are not spherical or that there is some size polydispersity. It should be noted that it is not possible to differentiate between the two effects.[35] Introducing polydispersity alone for this particular sample (i.e., assuming that all the scatterers are spherical and that the distribution is Gaussian), the polydispersity index of the radius was found to be equal to 1.02 (for R_{sc} = 48 Å). However, polydispersity and/or nonsphericity appears to depend very much on the sample history; furthermore, for some molecular architecture (long PS blocks and short ionic blocks) the characteristic oscillations could hardly be detected. Although the first-order correlation peak was quite intense and narrow, no more than two higher order maxima could ever be detected. Thus, the available information was not sufficient to determine a lattice symmetry. Consequently, model fitting of the complete scattering profiles was deliberately not used as it required the introduction of too many parameters and was not selective enough.

Since the position of the first correlation peak can be determined with precision, Bragg's law was boldly applied to obtain a characteristic length, denoted d_{Bragg}, which is proportional (but not necessarily equal) to the average center-to-center separation between the ionic domains. The effect of various parameters on this length was analyzed. Although the values of d_{Bragg} might not be exact, the relative variations are meaningful. Figure 3 represents the variation of the Bragg distance with the total number of units in the chain for a series of PS–P4VP·MeI triblock samples prepared by DMF casting. The lengths of the ionic and nonionic blocks were varied independently. Dotted lines connect data for constant midblock lengths, while solid lines connect data for samples, with similar end block lengths. It is clear that the end block has a far stronger effect than the midblock on the characteristic distance. For example, adding 10 ionic units increases the d_{Bragg} by ca. 25 Å; on the other hand, adding 10 PS units decreases d_{Bragg} only by ca. 1 Å. Since the rate of change of the Bragg distance is approximately the same as that of the ionic block length in its planar zigzag form, the result suggests that the end blocks are in a rather extended conformation, since d_{Bragg} can be thought of as a measure of the total end-to-end distance of the chain. The same general trend was observed for all the materials investigated and had already been noticed for the PS–P4VP·MeI molded samples.[27]

To obtain structural information, we proceeded as follows: First the domains were assumed to be spherical and arranged on some regular lattice of unknown symmetry; this starting hypothesis is justified both by the available experimental data on this system (presence of structure peaks and form factors) and by analogy with the known structure of nonionic block copolymers at a low volume fraction of one of the components, e.g., spherical microdomains on a body-centered cubic lattice. Complete phase separation and negligible interphase thickness were also assumed, which is reasonable in view of the strong incompatibility between ionic and nonionic segments. This is also supported by an asymptotic q^{-4} dependence of the scattering intensity at large angles, as shown in the previous paper.[31] Knowing the position of the first diffraction peak (q_{max}) and the volume fraction of the ionic microdomain (Φ_A),[36] as dictated by the molecular architecture, it is possible, using simple crystallographic, geometric, and space-filling calculations, to compute a radius of the spheres. For a simple cubic lattice, for instance, the radius

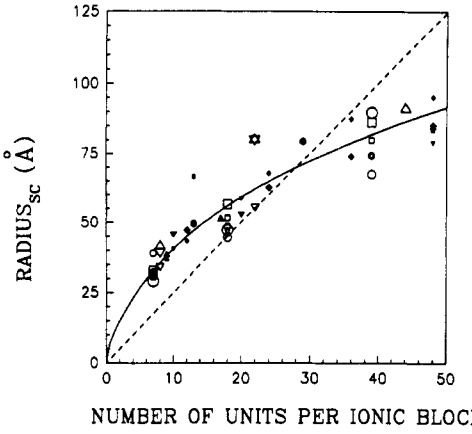

Figure 4. Radius of spherical ionic domains as a function of number of units per end block for a range of different materials. The values are those obtained by space-filling calculations (see text). The full line is a guide for the eye; the dotted line shows the extended length of the average end block. The increasing symbol sizes represent the different methods of preparation, methods 1–4, respectively.

is expressed as

$$R = \left[\frac{3.90}{q_{max}}\right]\Phi_A^{1/3} \quad (1)$$

Other quantities can also be calculated, such as the center-to-center distance (d), the surface-to-surface separation between the spheres (d'), the aggregation number (N), and the contact area (S/N), defined as the interphase area divided by the number of chains in a sphere. These are, evidently, not independent but are useful to obtain a better insight into the morphology. The calculations were performed for simple cubic (sc), body-centered cubic (bcc), and face-centered cubic (fcc) lattices. The different lattices give comparable values of the radii. For example, for the P(S-*b*-CsMA) copolymer labeled 18–440 prepared with method 3 (see Table I), the results are R_{sc} = 51 Å, R_{bcc} = 56 Å, and R_{hcp} = 45 Å (of spheres on a hexagonal close packed lattice).

The values of the radii were then compared to those calculated from the experimental form factor, when available. It is worth recalling that for monodisperse spheres, the intensity due to the form factor is related to R by

$$I(q) \cong \left[3\frac{\sin(qR) - qR\cos(qR)}{(qR)^3}\right]^2 \quad (2)$$

and this equation was used in Figure 2 to generate the shape factor plot for the same sample (18–440). The value of R is 48 Å. The agreement, similar for all samples, is good in view of the approximations involved in the space-filling calculations.

Figure 4 represents the radius of the spherical domains as a function of the number of repeat units per ionic block. The R_{sc} values obtained from space-filling calculations were selected, since the sc lattice gave values which compared best with those obtained from the shape factor peaks, when available. It does not imply, however, that this is the observed lattice. Samples shown in Figure 4 contain di- and triblocks prepared by the methods listed in Table I. For these materials, the length of the nonionic block ranges from 200 to 1000 units. The striking evidence is that all values fall on the same curve. This shows that the radius of the ionic domains is independent of all the other parameters that were varied in this set of samples. The fully stretched zigzag length of the ionic blocks, obtained by multiplying the number of units per ionic block by 2.5 Å, is also given. It can be seen that, at least up to a certain length of the ionic blocks, the radius of the ionic domains is of the order of the fully stretched length of the ionic blocks.

Table II. Relevant Parameters, Obtained from Space-Filling Calculation Assuming a Simple Cubic Lattice, for the Samples Prepared with Methods 1 and 2

	R_{sc} (Å) method[b]		d'[c] (Å) method		N[d] method		S/N[e] method		$\langle r_0^2\rangle^{1/2}$[f]
sample	1	2	1	2	1	2	1	2	(Å)
4VP·MeI–Styrene									
10–200–10[b]	41	46	47	52	110	160	190	170	110
20–200–20	59	53	36	32	170	120	260	290	
13–260	67	50	130	93	370	150	150	200	90
29–260	120	79	120	83	910	280	190	280	
9–480–9	37	38	84	86	93	100	190	180	
17–480–17	52	51	76	76	130	130	250	260	180
48–480–48	83	84	50	51	200	210	440	440	
12–960–12	43	47	120	130	110	140	210	200	
24–960–24	68	62	130	120	210	170	270	300	250
36–960–36	87	74	120	110	300	180	320	370	
48–960–48	95	85	110	100	290	210	390	430	
CsMA–Styrene Neutralized in Dioxane									
7–440	33	31	140	120	100	83	130	140	
18–440	47	51	130	120	120	150	240	220	120
39–440	74	80	130	120	210	260	330	300	

[a] $R_{sc} = [3.90/q_{max}]\Phi_A^{1/3}$. [b] Same signification as in Table I. [c] $d' = d - 2R_{sc}$. [d] Number of chains per domain. [e] (Surface area)/(no. of chain ends). [f] Unperturbed end-to-end distance of corresponding polystyrene chain (B for ABA and AB).

The following explanation can be given for the high extension observed. The surface energy between the ionic and nonionic phase is very high, which suggests that the system will tend to maximize the size of the spheres to minimize the surface area between the phases. This proceeds until the entropic cost of stretching the ionic chains is balanced by the surface energy gained through an increase in the radius of the spheres. Indeed, for the longer ionic chains, departure from the planar zigzag value is observed in the figure. For the shortest ionic sequences, the extension entropy is low and the radius of the sphere is of the order of the zigzag length of the ionic sequence. This does not mean that all the chains are fully extended since, obviously, this would lead to packing problems. It is rather believed that some chains may be fully extended, fixing the diameter of the spheres, while some others are less extended in order to fill the spherical space. Polydispersity of the ionic block is also relevant and is now under study.[37] Indirect evidence suggests that, for the materials used in this work, it is of the order of 1.3.[30]

The various parameters obtained from the space-filling calculations for a simple cubic lattice, i.e., R_{sc}, d', N, and S/N, along with the unperturbed end-to-end distance of the corresponding free polystyrene chain ($\langle r_0^2\rangle^{1/2}$), are summarized in Table II for samples with $\Phi_A < 0.2$ prepared by methods 1 and 2. The other methods of preparation are not reported, since the calculated parameters would have shown the same trends. The fact that the free distance (d') is always smaller than $\langle r_0^2\rangle^{1/2}$ should be compared to the results of a recent investigation by SANS, using selective deuteration of the styrene–4-vinylpyri-

dinium ABA compression-molded ionomer, which has shown that the polystyrene chain has, on average, its unperturbed dimension.[31] As expected, most chains do not link nearest neighbor domains but reach out further. The contact surface area, S/N, is somewhat smaller than is usually observed in nonionic block copolymers, also illustrating the fact that the interfacial energy is high. Due to the observed dependence of the radius on the molecular weight for the short ionic segments, N varies as the second power of the molecular weight of the ionic segment, and S/N is approximately constant in that range.

Finally, a comment concerning sources of error is in order. While the shape factors give sizes directly, polydispersity or deviations from sphericity smear out the features[35] and thus introduce an inherent uncertainity into the results. For some samples, the oscillations in intensity are not even visible. In view of the fact that the polydispersity of sphere radii as determined from the shape factor features is large, we estimate the precision of the value of radius to be no better than 10%. The calculations of domain size derived from the position of the first correlation peak relies on assumptions concerning the applicability of Bragg's law and the existence of a pseudocrystalline lattice. The deduced values have been considered as reliable only because they agreed, within experimental error, with those obtained directly, when available. Consequently, a set of values was available, which gave us information on the variation of the domain sizes as a function of the investigated parameters. When visible (rarely), the second-order intensity maximum appeared at a wave vector ranging from 1.7 to 1.9 times that of the first-order maximum. This would correspond to a hcp lattice. However, given the width of the peak, the structure appeared to be akin to that of amorphous glasses. To distinguish between the two possibilities, a comprehensive investigation was performed to determine the structure of solutions of the AB diblock ionomers from dilute to concentrated (gels) regimes.[38] This study should provide some insights on the exact structure of these samples.

Conclusions

The ionic block copolymers represent an excellent system for the investigation of the effect of very high incompatibility on the morphology of block copolymers. Because of this incompatibility, even very short ionic blocks are phase separated and produce a spherical morphology. The sizes of the phase-separated domains were obtained from the SAXS profile for two independent methods. The first method involves the use of the shape factor profiles for spherical domains, which gives the size directly. In the other method, the sizes are deduced from space-filling calculations, using the structure factor peak and assuming a simple cubic lattice. Agreement with the first method is within experimental error.

It is concluded that the sizes of the ionic microdomains are independent of the length of the nonionic blocks, their chemical nature, their architecture, or the sample preparation methods used in this study. In contrast to the polystyrene chains which have their unperturbed dimensions,[31] the ionic blocks are extended in their microdomains in order to reduce the total interfacial area. The primary factor which governs the behavior of these systems is the high degree of incompatibility rather than the ionic nature of one of the phases. From the point of view of ionomeric materials, the ionic aggregates can be described as supermultiplets.

Acknowledgment. This work was supported by the N.S.E.R.C. (Canada) and by a N.A.T.O. collaborative travel grant (0504/86). J.-P.G. is grateful to N.S.E.R.C. for postgraduate fellowship. The authors also thank A. Desjardins for the preparation of some of the materials used in this work. Constructive comments from one of the referees is gratefully acknowledged.

References and Notes

(1) Eisenberg, A. *Macromolcules* **1970**, *3*, 147. Eisenberg, A.; King, M. *Ion-Containing Polymers*; Academic Press: New York, 1977.
(2) Marx, C. L.; Caulfield, D. J.; Cooper, S. L. *Macromolecules* **1973**, *6*, 344.
(3) Holliday, L., Ed. *Ionic Polymers*; Halsted-Wiley: New York, 1975.
(4) Bazuin, C. G.; Eisenberg, A. *Ind. Eng. Chem. Prod. Res. Dev.* **1981**, *20*, 271.
(5) MacKnight, W. J.; Earnest, T. R. *J. Polym. Sci., Macromol. Rev.* **1981**, *16*, 41.
(6) Longworth, R. In *Developments in Ionic Polymers—1*; Wilson, A. D., Prosser, H. J., Eds.; Applied Science: London, 1983; Chapter 3.
(7) Feng, D.; Venkateshwaran, L. N.; Wilkes, G. L.; Leir, C. M.; Stark, J. E. *Polym. Mater. Sci. Eng.* **1988**, *58*, 999.
(8) Estes, G. M.; Cooper, S. L. *J. Macromol. Sci., Macromol. Chem.* **1970**, *C4* (2), 313.
(9) *Colloidal and Morphological Behavior of Block* and *Graft Copolymers*; Molau, G. E., Ed.; Plenum: New York, 1971.
(10) *Block and Graft Copolymerization*; Ceresa, R. J., Ed.; Wiley: New York, 1972.
(11) Noshay, A.; McGrath, J. E. *Block Polymers*; Academic Press: New York, 1977.
(12) *Block Polymers*; Aggarwal, S. L., Ed.; Plenum: New York, 1979.
(13) *Developments in Block Copolymers—1*; Goodman, I., Ed.; Applied Science: London, 1982.
(14) *Developments in Block Copolymers—2*; Goodman, I., Ed.; Elsevier Applied Science: London, 1985.
(15) Williams, C. E. In *Contemporary Topics in Polymer Science: Multiphase Macromolecular Systems*; Culbertson, B. M., Ed.; Plenum Press: New York, 1989; Vol. 6. Williams, C. E.; Russell, T. P.; Jérôme, R.; Horrion, J. *Macromolecules* **1986**, *19*, 2877.
(16) Schindler, A.; Williams, J. L. *Polym. Prepr. (Am. Chem. Soc., Div. Polym. Chem.)*. **1969**, *10* (2), 832.
(17) Fielding-Russel, G. S.; Pillai, P. S. *Polymer* **1977**, *18*, 859.
(18) Isono, Y.; Tanisugi, H.; Endo, K.; Fujimoto, T.; Hasegawa, H.; Hashimoto, T.; Kawai, H. *Macromolecules* **1983**, *16*, 5.
(19) Gauthier, S.; Eisenberg, A. *Macromolecules* **1987**, *20*, 760.
(20) Stadler, R.; Moeller, M.; Burgert, J.; Omeis, J.; de Lucca Freitas, L. In *Integration of Fundamental Polymer Science and Technology II*; Kleintjens, L. A., Lemstra, P. J., Eds.; Elsevier Applied Science: London, 1987; p 94.
(21) Storey, R. F.; George, S. E. *Polym. Mater. Sci. Engl.* **1988**, *58*, 985.
(22) Jacovic, M. S.; Favier, J. C.; Janah, H. *Makromol. Chem., Rapid Commun.* **1989**, *10*, 217.
(23) Allen, R. D.; Yilgor, I.; McGrath, J. E. In *Coulombic Interactions in Macromolecular Systems*; Eisenberg, A., Bailey, F. E., Eds.; ACS Symposium Series 302; American Chemical Society: Washington, DC, 1986; p 79. Long, T. E.; Allen, R. D.; McGrath, J. E. In *Chemical Reactions on Polymers*; Benham, J. L., Kinstle, J. F., Eds.; ACS Symposium Series 364; American Chemical Society: Washington, DC 1988; p 258. Storey, R. F.; George, S. E. In *Multiphase Polymers: Blends and Ionomers*; Utraki, L. A., Weiss, R. A., Eds.; ACS Symposium Series 395; American Chemical Society: Washington, DC, 1989; p 330.
(24) Weiss, R. A.; Sen, A.; Pottick, L. A.; Willis, C. L. *Polym. Commun.* **1990**, *31*, 220.
(25) Venkateshwaran, L. N.; York, G. A.; Deporter, C. D.; Long, T. E.; McGrath, J. E.; Wilkes, G. L. *Polymer* **1992**, *33* (11), 2277.
(26) Leemans, L.; Fayt, R.; Teyssié, Ph.; Jaeger, N. C. *Macromolecules* **1991**, *24*, 5922.
(27) Gouin, J. P.; Williams, C. E.; Eisenberg, A. *Macromolecules* **1989**, *22*, 4573.
(28) Selb, J.; Gallot, Y. In *Developments in Block Copolymers—2*; Goodman, I., Ed.; Elsevier Applied Science: London, 1985; Chapter 2.
(29) Desjardins, A.; Eisenberg, A. *Macromolecules* **1991**, *24*, 5779.
(30) Zhong, X. F.; Varshney, S. K.; Eisenberg, A. *Macromolecules* **1992**, *25*, 7160.
(31) Gouin, J. P.; Williams, C. E.; Eisenberg, A. *Macromolecules* **1992**, *25*, 1368.

(32) Wollmann, D.; Williams, C. E.; Eisenberg, A. *J. Polym. Sci., B: Polym. Phys.* **1990**, *28*, 1979.

(33) Desjardins, A. Ph.D. Thesis, McGill University, 1992.

(34) Dubuisson, J. M.; Dauvergne, J. M.; Depautex, C.; Vachette, P.; Williams, C. E. *Nucl. Instrum. Methods Phys. Res.* **1986**, *A246*, 636.

(35) Glatter, O.; Kratky, O. In *Small Angle X-Ray Scattering*; Academic Press: New York, 1982.

(36) The volumes of the polymer units were calculated with the following densities (ρ): $\rho_{PS} = 1.05$ g/cm^3, $\rho_{P(4VP\cdot MeI)} = 1.60$ g/cm^3, and $\rho_{P(C_8MA)} = 1.75$ g/cm^3.

(37) Nguyen, D.; Williams, C. E.; Eisenberg, A., in preparation.

(38) Nguyen, D.; Williams, C. E.; Eisenberg, A., in preparation.